



Efficiency of the interfacial charge transfer complex between TiO₂ nanoparticles and caffeic acid against DNA damage *in vitro*: A combinatorial analysis

VESNA LAZIĆ¹, IVANA VUKOJE¹, BOJANA MILIĆEVIĆ¹, BILJANA SPREMO-POTPAREVIĆ², LADA ŽIVKOVIĆ², DIJANA TOPALOVIĆ², VLADAN BAJIĆ¹, DUŠAN SREDOJEVIĆ¹ and JOVAN M. NEDELJKOVIĆ^{1*}

¹Vinča Institute of Nuclear Sciences, University of Belgrade, P.O. Box 522, Serbia

²Department of Physiology, Faculty of Pharmacy, University of Belgrade, Serbia

(Received 17 December 2018, revised 25 February, accepted 26 February 2019)

Abstract: The genotoxic and antigenotoxic behavior of the interfacial charge transfer (ICT) complex between nano-sized TiO₂ particles and caffeic acid (CA) was studied in *in vitro* experiments. The formation of the ICT complex is indicated by the appearance of absorption in visible-spectral range. The continual variations method indicated bridging coordination between the ligand, caffeic acid, and the surface Ti atoms, while the stability constant of the ICT complex was found to be 1.5×10^3 mol⁻¹ L. An agreement between the experimental data and the theoretical results, based on the density functional theory, was found. The ICT complex and its components did not display genotoxicity in the broad concentration range 0.4–8.0 mg mL⁻¹ TiO₂ at a mole ratio $c(\text{TiO}_2)/c(\text{CA}) = 8$. On the other hand, post-treatment of damaged DNA by the ICT complex induced antigenotoxic effect at lower concentrations, but at higher concentrations, 5.125–10.250 mg mL⁻¹ ICT, the ICT complex did not show any beneficial effect on H₂O₂-induced DNA damaged cells. The experimental data were analyzed using the combinatorial method to determine the effect of component interaction on the genotoxic and antigenotoxic behavior of the ICT complex.

Keywords: hybrid nanomaterials; DFT calculation; genotoxic property; anti-genotoxic property.

INTRODUCTION

Titanium dioxide (TiO₂) has been extensively studied due to its potential applications in diverse fields, such as environmental remediation, hydrogen production, medicine, food and cosmetic industry, sensors, *etc.*^{1–3} However, the enormous development of nanotechnology leads to increased release of nanoparticles (NPs) into the environment and raised justifiable issues concerning their

* Corresponding author. E-mail: jovned@vin.bg.ac.rs
<https://doi.org/10.2298/JSC181217017L>

toxicity.^{4–8} However, reports concerning the genotoxicity of TiO₂ NPs are controversial. On the one hand, a number of reports indicated toxicity of TiO₂ NPs due to their ability to induce oxidative stress through the production of reactive oxidative species,^{9–12} while, on the other hand, genotoxic effects of TiO₂ NPs were not found in the *in vitro* comet assay, bacterial and mammalian cell mutation tests, chromosomal aberration assay, and even in *in vivo* micronucleus assays.^{13–15} Most likely, the disagreement between these results is a consequence of the different methods of synthesis used, different size of TiO₂ NPs, different administration routes, *etc.*^{16–18}

Recently, the formation of interfacial charge transfer (ICT) complexes, facilitated by a polycondensation reaction between hydroxyl groups originating from the surface of TiO₂ and small organic molecules have been reported.^{19–22} In such hybrid structures, localized orbitals of the surface-attached ligands are electronically coupled with the delocalized electron levels from the conduction band of the TiO₂ semiconductor. Consequently, absorption of light by the ICT charge-transfer (CT) complex results in the excitation of electrons from the chelating ligand directly into the conduction band of TiO₂ nanocrystallites. The most striking feature of the formation of an ICT complex is the red shift of the absorption onset and, consequently, the appearance of absorption in more practical visible or near infrared spectral region. Strong ICT transitions have been reported between TiO₂ (colloidal NPs, mesoporous and commercial powders) and aromatic compounds with either two adjacent hydroxyl groups (catecholate-type of ligands)²³ or adjacent hydroxyl and carboxyl groups (salicylate-type of ligands),²⁰ as well as organic mono-hydroxyl compounds.²⁴ Naturally, there are few reports concerning the formation of ICT complexes with ligands that do not belong to phenolate-, catecholate- and salicylate-type, such as ascorbic acid,^{19,22} thiosalicylic acid²⁵ and hydrazine.²⁶ Until recently, research in this field was primarily motivated towards improved efficiency of photo-driven catalytic processes, such as degradation of organic polluters and water splitting reaction^{27,28} by taking advantage of the enhanced light-harvesting ability of inorganic–organic hybrid materials.

Although frequently the organic components of ICT complexes are biologically active molecules, *i.e.*, antioxidants such as ascorbic acid, caffeic acid, salicylic acid, *etc.*, there is only limited information concerning their influence on the toxicity of metal oxide particles. Hitherto, the antioxidant properties and efficiency against DNA damage of surface-modified TiO₂ NPs with ascorbic acid were studied in *in vitro* experiments,²² and the influence of caffeic acid on the acute toxicity of orally administered TiO₂ NPs was studied in *in vivo* experiments with mice.²⁹

The present study is a continuation of efforts to understand the genotoxic and antigenotoxic properties of inorganic–organic hybrid NPs. The ICT complex

between nanometer-sized TiO_2 particles and caffeic acid (CA) was thoroughly characterized by their composition, stability constant, and optical properties. The experimental data were supported by quantum chemical calculations based on the density functional theory (DFT). Special attention was paid to the genotoxic and antigenotoxic properties of the ICT complex and its components. The level of DNA damage in whole blood cells was evaluated in *in vitro* experiments by the comet assay method. A theoretical model, developed to analyze the dose-effect for multicomponent drug systems,³⁰ was, for the first time, applied to determine the combinatorial effect of the organic and inorganic component of an ICT complex on their genotoxic and antigenotoxic behavior over a broad concentration range.

EXPERIMENTAL

Synthesis and characterization of surface-modified TiO_2 NPs with CA

All employed chemicals were of high grade and used without additional purification (Aldrich, Fluka). Milli-Q deionized water (resistivity 18.2 m Ω cm) was used as a solvent. The TiO_2 colloids were prepared by dropwise addition of titanium(IV) chloride to cooled water as described elsewhere.³¹ The concentration of TiO_2 (0.165 mol L⁻¹) was determined from the concentration of the peroxide complex generated after dissolving the colloid in concentrated H_2SO_4 .³²

The formation of the ICT complex between TiO_2 NPs and CA is indicated by the immediate coloration of the colloid upon the addition of the ligand to the colloid. Due to enhanced particle–particle interaction upon surface modification, which eliminates the surface charges, precipitation or “gelling” of the colloid may occur. To avoid these problems, the pH of the solution was adjusted to 2 by diluting the TiO_2 colloids with an aqueous solution of HCl. According to pK_a value, the carboxylic group is more than 90 % in the protonated form at pH 2. The Benesi–Hildebrand spectrophotometric method was used for the determination of the stability constant of an ICT complex.^{33,34} The absorption spectra were recorded at room temperature using a Thermo Scientific Evolution 600 UV/Vis spectrophotometer.

For uniform TiO_2 particles, the molar concentration of the surface Ti atoms $c(\text{Ti}_{\text{surf}})$ could be calculated using the following equation:³⁵

$$c(\text{Ti}_{\text{surf}}) = 12.5c(\text{TiO}_2)/D \quad (1)$$

where $c(\text{TiO}_2)$ is the molar concentration of TiO_2 colloid and D is the size of particles in Å. Determination of stability constant is explained in details in a previous work.²²

The continual variations method (Job's method)³⁶ was applied for the spectrophotometric determination of the composition of the ICT complex. Solutions were prepared by mixing different volumes of equimolar solutions of Ti_{surf} and CA (2×10^{-3} mol L⁻¹). Briefly, a series of solutions were prepared in which the sum of the total concentration of Ti_{surf} and CA was constant (2×10^{-3} mol L⁻¹), but their proportions were varied. The volume of the TiO_2 solution varied from 1 to 9 mL, while those of the modifiers from 9 to 1 mL, with the total volume always being 10 mL.

The optical properties of ICT complex between TiO_2 NPs and CA were obtained by quantum chemical calculations based on the density functional theory (DFT) and time-dependent DF theory (TD-DFT). Details are given in Supplementary material to this paper.

Genotoxic and antigenotoxic potential of the ICT complex and its components

Whole blood samples with heparin were obtained from six healthy volunteers (two males and four females; ages: 20–30). All subjects who participated in this study were non-smokers and negated any use of alcohol, medications, supplements, nor were they receiving any therapy at the time of the study. Participants gave their consent in accordance with the regulations of the ethical standards of the Ethics Committee for Clinical Trials of the Faculty of Pharmacy, University of Belgrade. The collected blood samples (1 mL per subject) were immediately used in the *in vitro* comet assay in order to evaluate the genotoxic and antigenotoxic properties.

To evaluate concentration-dependent genotoxic and antigenotoxic effects of the ICT complex (CA/TiO₂) and its components (CA and unmodified TiO₂ NPs) over a wide concentration range, series of solutions were prepared in phosphate buffer saline (PBS); CA (0.1125, 0.2250, 0.3375, 1.125 and 2.250 mg mL⁻¹), unmodified TiO₂ NPs (0.4, 0.8, 1.2, 4.0 and 8.0 mg mL⁻¹), and CA/TiO₂ with constant mole ratio between components ($c(\text{TiO}_2)/c(\text{CA}) = 8$; for example, 0.4 mg mL⁻¹ TiO₂ + 0.1125 mg mL⁻¹ CA, etc.). The samples of peripheral blood (6 µL) were suspended in 0.67 % low melting point (LMP) agarose and spread over microscope slides. The coverslips were placed over them to distribute the sample evenly, after which the slides were cooled for 5 min at 4 °C in order for the agarose to solidify. After removing the coverslips, for the determination of the genotoxic potential of examined samples, whole blood cells were exposed to the examined samples for 1 h at 37 °C. Following the treatment, samples were covered with a layer of 0.5 % LMP agarose and re-cooled for 5 min at 4 °C. The effects were compared with a control sample, *i.e.*, whole blood cells treated only with the PBS solution. It should be noted that the surface-modified TiO₂ colloids with CA were combined with PBS solutions. The prepared CA/TiO₂–PBS mixtures were used immediately to avoid agglomeration of the nanoparticles.

For determination of the antigenotoxic properties of the ICT complex and its components, the samples of whole blood cells were first treated with 50×10⁻⁶ mol L⁻¹ H₂O₂ for 15 min on ice in order to expose the cells to an oxidant and therefore causing oxidative DNA damage. Subsequently, cells were rinsed with PBS and exposed for 1 h at 37 °C to the previously described set of solutions. The protective effects were compared with control, *i.e.*, the cells exposed to 50×10⁻⁶ mol L⁻¹ H₂O₂. Fifty µM H₂O₂ was chosen for the control, since this was the smallest concentration that produced a significant level of DNA damage in the treated cells as compared to the untreated controls, while also retaining good cell viability (data not shown).

The viability of cells used in the different treatments was checked with the Trypan Blue exclusion method. For the estimation of the fraction of dead cell, the cell samples were stained with a 0.4 % solution of Trypan Blue in PBS. The number of blue-stained (dead) cells within 2,000 cells was counted on a hemocytometer. The cell viability was above 90 %.

The level of DNA damage was evaluated by the comet assay method. The slides with whole blood cells were prepared as mentioned above and gel electrophoresis was performed as described elsewhere.³⁷ Briefly, after solidification, the slides were immersed in a cold lysing solution in plastic jars overnight at 4 °C, permitting the lysis of the cellular membranes and proteins. The following day, the slides were placed in the horizontal gel electrophoresis tank (CHU2 Manufacturer, connected to a power supply EPS 601) and submerged in cold fresh electrophoresis buffer (300×10⁻³ mol L⁻¹ NaOH, 10⁻³ mol L⁻¹ EDTA) allowing the DNA to unwind before electrophoresis. After 30 min, electrophoresis was conducted in dimmed light at 25 V and 300 mA for 30 min. Following electrophoresis, the slides were removed

from the tank and washed three times with neutralizing buffer at 5 min intervals and the final wash was performed with distilled water. The slides were then stained with 50 µL of ethidium bromide (20 mg mL⁻¹). After 15 min, the level of DNA damage was assessed by visual scoring of “comet-shaped nucleoids” on slides by a single well-trained scorer. One hundred randomly selected nuclei (50 nuclei from each of 2 replicate slides) were analyzed for each concentration at 100b× magnification using a fluorescence microscope Olympus BX50 (Olympus Optical, Hamburg, Germany), equipped with a mercury lamp HBO (50W, 516–560 nm, Zeiss). The cells were visually graded into 5 classes depending on the extent of DNA damage as described by Anderson *et al.*³⁸ 1) class A undamaged cells (<5 % damaged DNA); 2) class B: low-level damage (5–20 %); 3) class C: medium-level damage (20–40 %); 4) class D: high level damage (40–95 %); 5) class E: total destruction (>95 %). DNA damage was characterized as the number of cells from the DNA migration; 100 cells per sample were estimated. The data are expressed as the mean values with standard deviations. The statistical analysis was performed using an analysis of variance (one-way ANOVA), with Tukey’s post hoc test for comparisons of different treatments vs. the respective controls. A difference at * <0.05 was considered to be statistically significant.

Calculation of combinatorial genotoxic and antigenotoxic effects

The combinatorial effects of components of the ICT complex (CA and unmodified TiO₂ NPs) on genotoxic and antigenotoxic effects of the CA/TiO₂ were assessed from the measured concentration–effect relationships. The combination index (*CI*) allows quantitative determination of component interactions, where *CI* values (<1, ≈1 and >1) indicate synergism, additive effect, and antagonism, respectively. The *CI* values were calculated based on the linearized form of the median–effect equation derived from the mass–action law principle:³⁰

$$\log \frac{f_a}{1-f_a} = m \log D - m \log D_m \quad (2)$$

where *D* is the concentration of a component, *f_a* is the fraction of cells affected by *D*, *D_m* is the concentration that affects the system by 50 %, and *m* is the coefficient signifying the shape of the concentration–effect relationship.³⁹

The *CI* values for two-component system affected at different levels, *x* / % = 100*f_a*/(1−*f_a*) can be calculated using data from linearized concentration–effect relationships using the following equation:³⁰

$$CI = \frac{D_x^M(\text{TiO}_2)}{D_x(\text{TiO}_2)} + \frac{D_x^M(\text{CA})}{D_x(\text{CA})} \quad (3)$$

where *D_x*^M is the concentration of a specific component in the mixture that exerts *x* / % effect, while *D_x* is the concentration of each component alone that exerts the same effect.

RESULTS AND DISCUSSION

Characterization of TiO₂ NPs surface-modified with CA

TiO₂ NPs, synthesized by the acidic hydrolysis of titanium(IV) chloride, have often been used and their microstructural properties were described in detail previously.²² The used colloid consists of uniform, nearly spherical anatase TiO₂ NPs with an average size of about 45 Å.

The absorption spectra of a solution of CA and sols of pristine/unmodified TiO_2 colloid and TiO_2 colloid surface-modified with CA in acidic media (pH 2), as well as photo-images of unmodified and surface-modified TiO_2 colloids, are shown in Fig. 1A. The absorption in the visible spectral range is the consequence of the formation of the ICT complex between Ti_{surf} and CA. The observed absorption red-shift is in agreement with reported data concerning ICT complexes between colloidal TiO_2 NPs and catecholate-type of ligands.⁴⁰

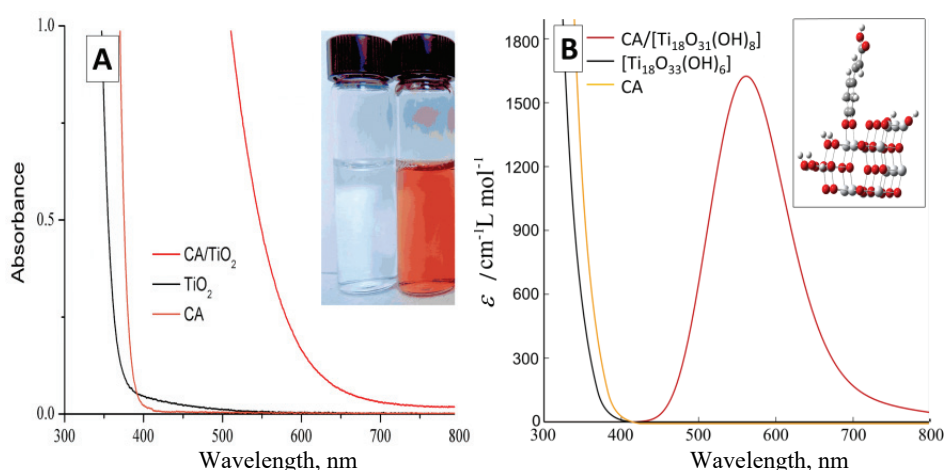


Fig. 1. A) Absorption spectra of 1×10^{-3} mol L⁻¹ CA, 2×10^{-3} mol L⁻¹ TiO_2 and CA/ TiO_2 with the same concentrations of components; inset: photo images of TiO_2 colloid unmodified and surface-modified with CA. B) The electronic excitation spectra of CA, $[\text{Ti}_{18}\text{O}_{31}(\text{OH})_8]$ cluster and CA/ $[\text{Ti}_{18}\text{O}_{31}(\text{OH})_8]$ cluster calculated by convolution with a full width at half maximum of 5000 cm^{-1} .

To complement the experimental data, the electronic excitation spectrum of CA/[$\text{Ti}_{18}\text{O}_{31}(\text{OH})_8$] cluster was calculated using TD-DFT. The constructed model of CA/[$\text{Ti}_{18}\text{O}_{31}(\text{OH})_8$] surface complex is based on dehydration reaction between two adjacent hydroxyl groups from CA and two hydroxyl group from the $[\text{Ti}_{18}\text{O}_{33}(\text{OH})_6]$ cluster. The optimized structure of CA/[$\text{Ti}_{18}\text{O}_{31}(\text{OH})_8$] cluster (see inset to Fig. 1B) indicates that the molecules of CA are almost perpendicularly attached to the surface of TiO_2 NPs. The calculated spectra of isolated CA molecule and $[\text{Ti}_{18}\text{O}_{33}(\text{OH})_6]$ cluster are in agreement with the corresponding measured spectra (see Fig. 1A), as well as calculated spectra reported in the literature.⁴¹ In addition, the absorption onset in the TD-DFT spectrum of the CA/[$\text{Ti}_{18}\text{O}_{31}(\text{OH})_8$] cluster is slightly red-shifted compared to the experimental one. However, the TD-DFT spectrum of CA/[$\text{Ti}_{18}\text{O}_{31}(\text{OH})_8$] cluster does not have absorption towards UV spectral region starting from 430 nm, while, of course, the measured spectra

have continuous broad absorption in UV spectral range. The reason for this discrepancy lies in the fact that a finite number of excitations was taken into account (first 30). A similar spectral shape with a dip around 450 nm was observed in a computational study concerning 2-anthroic acid adsorbed on a titania nanocluster.⁴²

The stability constant, K_b , was determined from the absorbances of a series of solutions (see Fig. 2.) having a fixed concentration of TiO_2 NPs ($c(\text{TiO}_2) = 10^{-3}$ mol L⁻¹, *i.e.*, $c(\text{Ti}_{\text{surf}}) = 0.28 \times 10^{-3}$ mol L⁻¹) and increasing concentrations of ligand ($c(\text{CA}) = 0.05 - 0.7 \times 10^{-3}$ mol L⁻¹). To avoid significant errors in the K_b determination, the wavelength of complex absorption was chosen to correspond to the optimal absorption range.³³ By plotting $1/A$ vs. $1/c(\text{CA})$, a straight line was obtained, and from the ratio of the intercept and the slope, the K_b value was found to be 1.5×10^3 mol⁻¹ L. The composition of the ICT complex – the stoichiometric ratio between $c(\text{Ti}_{\text{surf}})$ and $c(\text{CA})$ – was determined by the Job's method of continuous variation,³⁶ with the assumption that only one type of complex species is formed. The stoichiometric ratio between $c(\text{Ti}_{\text{surf}})$ and $c(\text{CA})$ was obtained by plotting the absorbance of the ICT complex *vs.* $x = c(\text{Ti}_{\text{surf}})/(c(\text{CA}) + c(\text{Ti}_{\text{surf}}))$. The Job's plot reached the maximum value at a mole fraction of $c(\text{Ti}_{\text{surf}})/(c(\text{CA}) + c(\text{Ti}_{\text{surf}}))$ of ≈ 0.65 , confirming that mole ratio between $c(\text{Ti}_{\text{surf}})$ and the ligand in the complex is 2:1 (see inset to Fig. 2). The determined stoichiometric mole ratio indicates bidentate bridging coordination of CA to the surface of TiO_2 NPs. This is in accordance with literature data and, also, the determined stability constant is of the same order of magnitude as the reported values for ICT complexes between colloidal TiO_2 NPs and various catecholate-type of ligands.⁴⁰

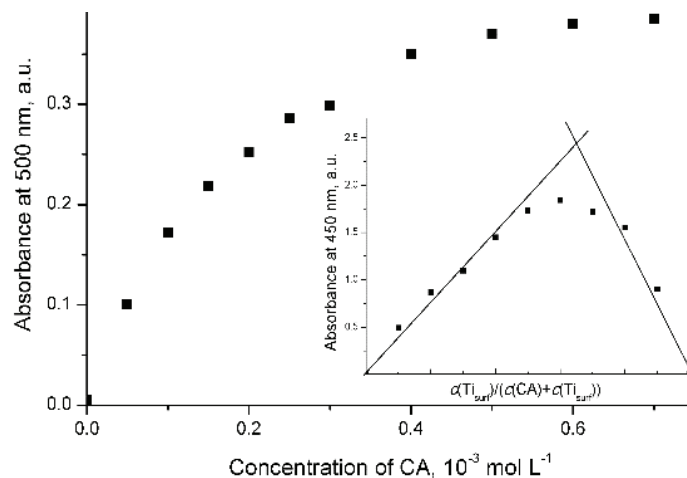


Fig. 2. Absorption at 500 nm of surface-modified TiO_2 with CA *vs.* modifier concentration (2×10^{-3} mol L⁻¹ TiO_2 , the data were recorded 2 h after surface modification); Inset: Job's curve of equimolar solutions for CA– Ti_{surf} complex ($c(\text{CA}) + c(\text{Ti}_{\text{surf}}) = 2 \times 10^{-3}$ mol L⁻¹).

Combinatorial effect on genotoxic and antigenotoxic properties of the ICT complex and its components

The results concerning genotoxicity and antigenotoxicity of free CA, unmodified TiO₂ colloid and surface-modified TiO₂ colloid with CA in whole blood cells, obtained *via* the comet assay, are presented in Tables I and II, respectively. The given values are average numbers of damaged DNA obtained out of 100 examined nuclei of six independent examinations. The standard deviations values are also included in Tables I and II. In order to examine concentration-dependent genotoxic and antigenotoxic effects of hybrid CA/TiO₂ NPs and its components, measurements were performed over a wide concentration range ($c(\text{TiO}_2)$, 0.4–8.0 mg mL⁻¹; mole ratio $c(\text{TiO}_2)/c(\text{CA}) = 8$).

TABLE I. The level of DNA damage in genotoxic experiments evaluated by the comet assay method for a series of CA solutions as well as unmodified and surface-modified TiO₂ colloids. The values of damaged DNA were obtained out of 100 examined nuclei and they are average of six independent examinations. The mole ratio between TiO₂ and CA in the ICT complexes was kept constant at 8; the level of DNA damage for PBS was 8.0±3.5

Caffeic acid					
Concentration, mg mL ⁻¹	0.1125	0.2250	0.3375	1.125	2.250
Number of damaged DNA nuclei	7.7±3.6	6.5±2.5	5.7±2.9	17.2±2.6	16.8±1.8
TiO ₂ colloid					
Concentration, mg mL ⁻¹	0.4	0.8	1.2	4.0	8.0
Number of damaged DNA nuclei	7.8±2.3	7.3±1.7	8.2±2.9	19.2±2.4	16.2±1.1
ICT complex					
Concentration, mg mL ⁻¹	0.5125	1.0250	1.5375	5.125	10.250
Number of damaged DNA nuclei	7.8±2.5	7.7±2.2	7.5±2.9	15.8±2.3	17.5±1.5

The results obtained by the comet assay indicate that in the tested concentration range, free CA, unmodified TiO₂ colloid, and surface-modified TiO₂ colloid with CA did not induce statistically significant increases of DNA damage compared to PBS, although, at higher concentrations, the number of damaged cells was 2–2.5 times larger compared to the lower concentrations. To put it simply, the ICT complex and its components are not genotoxic under the stated experimental conditions. CA is a well-known antioxidant with a strong reducing ability,⁴³ and, in addition, it did not exhibit genotoxicity in the comet assay experiments using concentrations that exceed the highest concentration in this study. However, the genotoxicity of TiO₂ NPs is still a matter of debate in the literature. Some reports indicated genotoxic effects of TiO₂ NPs due to its ability to induce the formation of reactive oxidative species that could interact with DNA,^{9,10} while, there are also reports showing no genotoxic action of TiO₂.^{13,14} On the other hand, there is a lack of information concerning the toxicity of inorganic–organic hybrid NPs.

Antigenotoxic effects in post-treatment experiments were examined in the same concentration range of the ICT complex and its components, and the results are given in Table II. The post-treatment with CA solution and unmodified TiO₂ colloid over the entire concentration range led to a significant decrease in the damaged DNA cells compared to the control. These results are in agreement with published data concerning the antigenotoxic effect of unmodified TiO₂ NPs,²² and antigenotoxic effect of CA.⁴³ Post-treatment with the ICT complex formed between TiO₂ and CA displayed antigenotoxic effect at lower concentrations (0.5–1.6 mg mL⁻¹ ICT; mole ratio $c(\text{TiO}_2)/c(\text{CA}) = 8$). However, at higher concentrations (>5 mg mL⁻¹ ICT; mole ratio $c(\text{TiO}_2)/c(\text{CA}) = 8$), the ICT complex showed no beneficial effect on H₂O₂ damaged cells. Most likely, the enhanced particle–particle interaction upon surface modification eliminates the surface charge, inducing precipitation and/or "gelling" of the colloidal NPs in whole blood samples. This might be the reason for the absence of an antigenotoxic effect of the ICT complex at high concentrations.

TABLE II. The level of DNA damage in the antigenotoxic experiments after the exposure to H₂O₂ evaluated by the comet assay method for a series of CA solutions as well as unmodified and surface-modified TiO₂ colloids. The values of damaged DNA were obtained out of 100 examined nuclei and the results are an average of six independent examinations. The molar ratio between TiO₂ and CA in the ICT complexes was kept constant at 8; the level of DNA damage for H₂O₂ was 29.7±1.7

	Caffeic acid				
Concentration, mg mL ⁻¹	0.1125	0.2250	0.3375	1.125	2.250
Number of damaged DNA nuclei ^a	11.5±2.4	12.0±3.2	11.7±3.1	19.5±2.0	20.2±3.8
TiO ₂ colloid					
Concentration, mg mL ⁻¹	0.4	0.8	1.2	4.0	8.0
Number of damaged DNA nuclei ^a	10.7±2.1	10.8±3.2	10.7±2.7	19.7±1.8	18.7±0.9
ICT complex					
Concentration, mg mL ⁻¹	0.5125	1.0250	1.5375	5.125	10.250
Number of damaged DNA nuclei ^a	11.7±1.6	14.3±2.1	14.3±2.7	29.7±8.8	28.3±2.9

^aDifference at $p < 0.05$ was considered statistically significant, versus the H₂O₂ treated control (by one-way ANOVA with Tukey's *post hoc* test Kruskal)

Combinatorial genotoxic and antigenotoxic effects of the inorganic and organic component that form the ICT complex were analyzed using a theoretical model design to analyze the dose-effect relationship for multicomponent drug systems.³⁰ This approach is based on the assumption that when two components/drugs are combined and subjected to serial dilutions, the combined mixture of the two components behaves as a third, independent entity. It should be emphasized that this analysis does not provide insight into the genotoxic and antigenotoxic mechanism of the investigated species, but provides a concentration range where they display either antagonistic or additive or synergistic behavior. The

experimental data collected in Tables I and II for concentration-dependent genotoxic and antigenotoxic behavior of the ICT complex and its components are introduced into Eq. (2) – a linearized form of the median-effect equation. Experimental data and their linear fits ($\log(f_a/(1-f_a))$ vs. $\log(c(\text{TiO}_2)+c(\text{CA}))$) are presented in Fig. 3 (A and B for genotoxic and antigenotoxic effect, respectively). A few points should be emphasized. First, Chou³⁰ suggested that the mixtures should have the same ratio of the components rather than non-constant ratios (*e.g.*, varying the concentration of the first component while keeping the concentration of the second one constant). Thus, the ICT complexes were prepared in the entire concentration range with a constant molar ratio between TiO_2 NPs and CA ($c(\text{TiO}_2)/c(\text{CA}) = 8$). Second, taking into account the stability constant of the ICT complex ($1.5 \times 10^3 \text{ mol}^{-1} \text{ L}$) the mole ratio between TiO_2 NPs and CA was chosen to avoid the significant presence of free ligand in the solution. Basically, this mole ratio leads to the formation of a sub-monolayer of CA on the surface of TiO_2 NPs. Finally, an increase of the population of affected DNA indicates an increase of an undesired genotoxic or antigenotoxic effect.

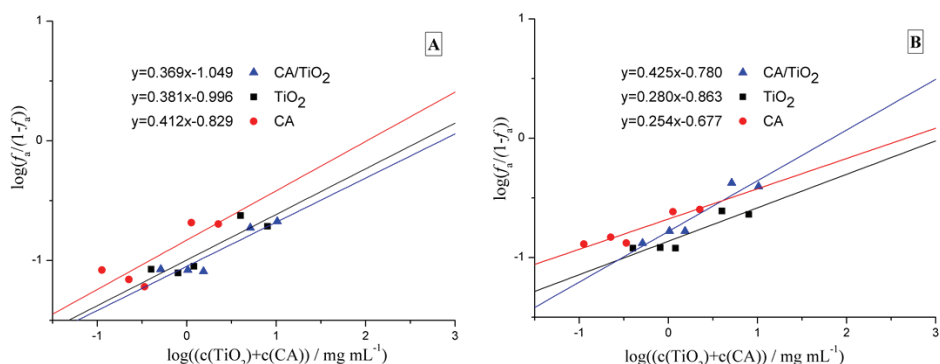


Fig. 3. A) Genotoxic and B) antigenotoxic concentration-effect plots for free CA, TiO_2 colloid and ICT complex between CA and TiO_2 ; the equation of the linear fits are given in insets.

In order to determine the *CI* values, *i.e.*, to determine the concentration ranges where components of hybrid CA/ TiO_2 NPs display either antagonistic, or additive or synergistic behavior, first, the concentration of each component alone that exerts an $x\%$ genotoxic or antigenotoxic effect ($D_x(\text{TiO}_2)$ and $D_x(\text{CA})$) and the concentration of components in the mixture that exerts the same effect ($D_x^M(\text{TiO}_2)$ and $D_x^M(\text{CA})$) were calculated from linear equations obtained by fitting the experimental data (see insets to Fig. 3A and B). These values were introduced into Eq. (3) in order to obtain the *CI* values (see Table III). Although combinatorial analysis has a predictive character and can be performed beyond the experimentally obtained data, the *CI* values were calculated in a relatively narrow range (from 5 to 25 % of the affected cells) in order to obtain meaningful characteristics

of the system under investigation. It should be noted that the ICT complex and its components do not display genotoxicity at low concentrations (almost identical to that of the PBS control), while, on the other hand, at the high concentration end, they do not display an antigenotoxic effect (the level of DNA damage is almost the same as for H₂O₂). Moreover, at concentrations exceeding the highest concentration of the ICT complex, the stability of the colloid was compromised.

TABLE III. Combination index (*CI*) values of the experimental mixtures that affect the percentage of cell population are indicated by the subscript number; according to Ref. (30): *CI* < 0.3 strong synergism, *CI* = 0.3–0.9 synergism, *CI* = 0.9–1.1 nearly additive, *CI* = 1.1–3.3 antagonism, *CI* > 3.3 strong antagonism

Genotoxicity – <i>CI</i> values				
<i>CI</i> ₅	<i>CI</i> ₁₀	<i>CI</i> ₁₅	<i>CI</i> ₂₀	<i>CI</i> ₂₅
1.667 antagonism	1.888 antagonism	2.048 antagonism	2.178 antagonism	2.294 antagonism
<i>D</i> _x ^M (TiO ₂) + <i>D</i> _x ^M (CA), mg mL ⁻¹				
0.186+0.052	1.408+0.395	4.934+1.388	12.688+3.568	27.679+7.784
Antigenotoxicity – <i>CI</i> values				
<i>CI</i> ₅	<i>CI</i> ₁₀	<i>CI</i> ₁₅	<i>CI</i> ₂₀	<i>CI</i> ₂₅
5.098 strong antagonism	1.820 antagonism	0.878 nearly additive	0.534 synergism	0.356 synergism
<i>D</i> _x ^M (TiO ₂) + <i>D</i> _x ^M (CA), mg mL ⁻¹				
0.052+0.015	0.500+0.140	0.904+0.243	2.054+0.578	4.042+1.139

The *CI* values for the combinatorial genotoxic effect of the components of the ICT complex indicate antagonism over the entire investigated range (from 5 to 25 % of affected cells). However, a different behavior was observed for the antigenotoxic effect. An increase of the concentration of the ICT complex induced changes from strong antagonism (*CI*₅) to antagonism (*CI*₁₀), over nearly additive (*CI*₁₅) to synergism (*CI*₂₀ and *CI*₂₅). It should be emphasized that the concentration-dependent genotoxic and antigenotoxic behavior of inorganic-organic hybrid nanoparticles has never previously been analyzed using theoretical model design to study the multiple drug-effect. Bearing in mind the diversity of bioactive ligands with the ability to form ICT complexes with various metal-oxides, it is important, in our opinion, to test the possibility of extending the application of this model to a field for which it was not originally designed.

CONCLUSION

Surface-modification of TiO₂ NPs with CA leads to the formation of a new chemical entity – an interfacial charge transfer complex. The composition, stability constant, and optical properties of the ICT complex were determined, as well as the mode of coordination between CA and surface Ti atoms. Experimental data were supported by quantum chemical calculations based on DFT. To

the best of our knowledge, the genotoxic and antigenotoxic potential of inorganic–organic hybrid CA/TiO₂ NPs has never been examined in *in vitro* experiments and compared with the genotoxic and antigenotoxic behavior of its constituents. The results obtained by the comet assay indicated that the ICT complex and its components are not genotoxic in the investigated concentration range. In addition, unmodified TiO₂ NPs and free CA display antigenotoxic behavior in the same concentration range. However, the hybrid CA/TiO₂ NPs display antigenotoxicity only at lower concentrations, while, when the concentration is sufficiently high, they do not have antigenotoxic properties. Most likely, at the high concentration end of ICT complex, the antigenotoxic properties of hybrid CA/TiO₂ NPs are compromised by their agglomeration in multi-component physiological fluid. The combinatorial effect of the components that constitute the ICT complex was analyzed using a theoretical model designed for multicomponent drug systems. The values of the combinatorial index determined at different levels of affected cells clearly indicated the range at which the components of the ICT complex display antagonistic, additive or synergistic behavior.

Acknowledgments. Financial support for this study was granted by the Ministry of Education, Science and Technological Development of the Republic of Serbia (Projects 45020 and 173034) and the hCOMET COST (Action No CA 15132).

ИЗВОД

УТИЦАЈ КОМПЛЕКСА СА ПРЕНОСОМ НАЕЛЕКТРИСАЊА ИЗМЕЂУ НАНОЧЕСТИЦА TiO₂ И КАФЕИНСКЕ КИСЕЛИНЕ НА ДНК ОШТЕЋЕЊЕ У *in vitro* ЕКСПЕРИМЕНТИМА: КОМБИНАТОРНА АНАЛИЗА

ВЕСНА ЛАЗИЋ¹, ИВАНА ВУКОЈЕ¹, БОЈАНА МИЛИЋЕВИЋ¹, БИЉАНА СПРЕМО-ПОТПАРЕВИЋ², ЛАДА ЖИВКОВИЋ², ДИЈАНА ТОПАЛОВИЋ², ВЛАДАН БАЈИЋ¹, ДУШАН СРЕДОЈЕВИЋ¹ и ЈОВАН М. НЕДЕЉКОВИЋ¹

¹Институција за нуклеарне науке "Винча", Универзитет у Београду, П.Ф.522, Београд и ²Клисегра за физиологију, Фармацевтски факултет, Универзитет у Београду, Београд

Генотоксична и антигенотоксична својства комплекса са преносом наелектрисања (ICT) између наночестица TiO₂ и кафеинске киселине су испитивана *in vitro* експериментима. Показано је да ICT комплекс апсорбује светлост у видљивом делу спектра. Методом континуалне варијације је утврђено да лиганд, кафеинска киселина, координише са површинским атомима Ti премошћавањем, при чему константа стабилности насталог комплекса износи $1.5 \times 10^3 \text{ mol}^{-1} \text{ L}$. Теоријски резултати, добијени коришћењем теорије функционала густине, су у сагласности са експерименталним резултатима. ICT комплекс и његове компоненте не показују генотоксичност у широком опсегу концентрација ($0.4\text{--}8.0 \text{ mg mL}^{-1}$ TiO₂; молски однос $c(\text{TiO}_2)/c(\text{CA}) = 8$). Са друге стране, накнадни третман оштећених ДНК ћелија ICT комплексом при ниским концентрацијама доводи до антигенотоксичног ефекта, док при високим концентрацијама ($5,125\text{--}10,250 \text{ mg mL}^{-1}$ ICT) не доводе до регенерације оштећених ДНК ћелија. Експериментални резултати су анализирани комбинаторном методом како би се утврдило међусобно дејство компонената на генотоксична и антигенотоксична својства ICT комплекса.

(Примљено 17. децембра 2018, ревидирано 25. фебруара, прихваћено 26. фебруара 2019)

REFERENCES

1. M. R. Hoffmann, S. T. Martin, W. Choi, D. W. Bahnemann, *Chem. Rev.* **95** (1995) 69 (<https://www.doi.org/10.1021/cr00033a004>)
2. S. Gunes, N. Marjanovic, J. M. Nedeljkovic, N. S. Sariciftci, *Nanotechnology* **19** (2008) 424009 (<https://www.doi.org/10.1088/0957-4484/19/42/424009>)
3. T. Rajh, N. M. Dimitrijevic, M. Bissonnette, T. Koritarov, V. Konda, *Chem. Rev.* **114** (2014) 10177 (<https://www.doi.org/10.1021/cr500029g>)
4. K. Donaldson, L. Tran, L. A. Jimenez, R. Duffin, D. E. Newby, N. Mills, W. MacNee, V. Stone, *Part. Fibre Toxicol.* **2** (2005) 10 (<https://www.doi.org/10.1186/1743-8977-2-10>)
5. S. P. Singh, M. F. Rahman, U. S. Murty, M. Mahboob, P. Grover, *Toxicol. Appl. Pharmacol.* **266** (2013) 56 (<http://dx.doi.org/10.1016/j.taap.2012.10.016>)
6. H. Bahadar, F. Maqbool, K. Niaz, M. Abdollahi, *Iranian Biomed. J.* **20** (2016) 1 (<http://www.ncbi.nlm.nih.gov/pmc/articles/PMC4689276/>)
7. J. Khalili Fard, S. Jafari, M. A. Eghbal, *Adv. Pharm. Bull.* **5** (2015) 447 (<https://www.ncbi.nlm.nih.gov/pubmed/26819915>)
8. A. Sukhanova, S. Bozrova, P. Sokolov, M. Berestovoy, A. Karaulov, I. Nabiev, *Nanoscale Res. Lett.* **13** (2018) 44 (<https://www.ncbi.nlm.nih.gov/pubmed/29417375>)
9. K. P. Lee, H. J. Trochimowicz, C. F. Reinhardt, *Toxicol. Appl. Pharm.* **79** (1985) 179 (<http://www.sciencedirect.com/science/article/pii/0041008X85903394>)
10. P. M. Hext, J. A. Tomenson, P. Thompson, *Ann. Occup. Hyg.* **49** (2005) 461 (<http://dx.doi.org/10.1093/annhyg/mei012>)
11. Z. Magdolenova, A. Collins, A. Kumar, A. Dhawan, V. Stone, M. Dusinska, *Nanotoxicology* **8** (2014) 233 (<https://www.ncbi.nlm.nih.gov/pubmed/23379603>)
12. H. Shi, R. Magaye, V. Castranova, J. Zhao, *Part. Fibre Toxicol.* **10** (2013) 15 (<https://doi.org/10.1186/1743-8977-10-15>)
13. V. Dunkel, E. Zeiger, D. Brusick, E. McCoy, D. McGregor, K. Mortelmans, H. S. Rosenkranz, V. F. Simon, *Environ. Mutagen.* **7** (1985) 1 (<https://doi.org/10.1002/em.2860070902>)
14. J. L. Ivett, B. M. Brown, C. Rodgers, B. E. Anderson, M. A. Resnick, E. Zeiger, *Environ. Mol. Mutagen.* **14** (1989) 165 (<https://www.onlinelibrary.wiley.com/doi/abs/10.1002/em.2850140306>)
15. T. Hasan, G. Fatime, *Toxicol. Ind. Heal.* **23** (2007) 19 (<https://doi.org/10.1177/0748233707076764>)
16. A. Churg, B. Gilks, J. Dai, *Am. J. Physiol.-Lung. C* **277** (1999) L975 (<https://www.physiology.org/doi/abs/10.1152/ajplung.1999.277.5.L975>)
17. J. Chen, X. Dong, J. Zhao, G. Tang, *J. Appl. Toxicol.* **29** (2009) 330 (<https://www.onlinelibrary.wiley.com/doi/abs/10.1002/jat.1414>)
18. A. Huk, A. R. Collins, N. El Yamani, C. Porredon, A. Azqueta, J. de Lapuente, M. Dusinska, *Mutagenesis* **30** (2015) 85 (<http://dx.doi.org/10.1093/mutage/geu077>)
19. T. Rajh, J. M. Nedeljkovic, L. X. Chen, O. Poluektov, M. C. Thurnauer, *J. Phys. Chem., B* **103** (1999) 3515 (<https://www.doi.org/10.1021/jp9901904>)
20. T. D. Savić, Z. V. Šaponjić, M. I. Čomor, J. M. Nedeljković, M. D. Dramićanin, M. G. Nikolić, D. Ž. Veljković, S. D. Zarić, I. A. Janković, *Nanoscale* **5** (2013) 7601 (<http://dx.doi.org/10.1039/C3NR01277H>)
21. I. M. Dugandžić, D. J. Jovanović, L. T. Mančić, O. B. Milošević, S. P. Ahrenkiel, Z. V. Šaponjić, J. M. Nedeljković, *Mater. Chem. Phys.* **143** (2013) 233 (<http://www.sciencedirect.com/science/article/pii/S0254058413006603>)

22. V. Bajić, B. Spremo-Potparević, L. Živković, A. Čabarkapa, J. Kotur-Stevuljević, E. Isenović, D. Sredojević, I. Vukoje, V. Lazić, S. P. Ahrenkiel, J. M. Nedeljković, *Colloids Surfaces, B Biointerfaces* **155** (2017) 323 (<http://www.sciencedirect.com/science/article/pii/S0927776517302187>)
23. C. Yang, H. Wu, J. Shi, X. Wang, J. Xie, Z. Jiang, *Ind. Eng. Chem. Res.* **53** (2014) 12665 (<http://dx.doi.org/10.1021/ie501734g>)
24. D. N. Sredojević, T. Kovač, E. Džunuzović, V. Đorđević, B. N. Grgur, J. M. Nedeljković, *Chem. Phys. Lett.* **686** (2017) 167 (<http://www.sciencedirect.com/science/article/pii/S0009261417307844>)
25. B. Milićević, V. Đorđević, D. Lončarević, J. M. Dostanić, S. P. Ahrenkiel, M. D. Dramičanin, D. Sredojević, N. M. Švrakić, J. M. Nedeljković, *Opt. Mater.* **73** (2017) 163 (<http://www.sciencedirect.com/science/article/pii/S0925346717305116>)
26. L. Tian, J. Xu, A. Alnafisah, R. Wang, X. Tan, N. A. Oyler, L. Liu, X. Chen, *Chemistry (Weinheim)* **23** (2017) 5345 (<https://www.doi.org/10.1002/chem.201606027>)
27. B. Milićević, V. Đorđević, D. Lončarević, S. P. Ahrenkiel, M. D. Dramičanin, J. M. Nedeljković, *Micropor. Mesopor. Mat.* **217** (2015) 184 (<https://doi.org/10.1016/j.micromeso.2015.06.028>)
28. S. Higashimoto, T. Nishi, M. Yasukawa, M. Azuma, Y. Sakata, H. Kobayashi, *J. Catal.* **329** (2015) 286 (<https://doi.org/10.1016/j.jcat.2015.05.010>)
29. D. Dekanski, B. Spremo-Potparević, V. Bajić, L. Živković, D. Topalović, D. N. Sredojević, V. Lazić, J. M. Nedeljković, *Food Chem. Toxicol.* **115** (2018) 42 (<http://www.sciencedirect.com/science/article/pii/S0278691518301388>)
30. T. C. Chou, *Pharmacol. Rev.* **58** (2006) 621 (<http://pharmrev.aspetjournals.org/content/58/3/621>)
31. T. Rajh, A. E. Ostafin, O. I. Micic, D. M. Tiede, M. C. Thurnauer, *J. Phys. Chem.* **100** (1996) 4538 (<https://doi.org/10.1021/jp952002p>)
32. G. Eisenberg, *Ind. Eng. Chem. Anal. Ed.* **15** (1943) 327 (<https://doi.org/10.1021/i560117a011>)
33. H. A. Benesi, J. H. Hildebrand, *J. Am. Chem. Soc.* **71** (1949) 2703 (<https://doi.org/10.1021/ja01176a030>)
34. W. B. Person, *J. Am. Chem. Soc.* **87** (1965) 167 (<https://doi.org/10.1021/ja01080a006>)
35. L. X. Chen, T. Rajh, Z. Wang, M. C. Thurnauer, *J. Phys. Chem., B* **101** (1997) 10688 (<https://doi.org/10.1021/jp971930g>)
36. W. C. Vosburgh, G. R. Cooper, *J. Am. Chem. Soc.* **63** (1941) 437 (<https://doi.org/10.1021/ja01847a025>)
37. N. P. Singh, M. T. McCoy, R. R. Tice, E. L. Schneider, *Exp. Cell Res.* **175** (1988) 184 (<http://www.sciencedirect.com/science/article/pii/0014482788902650>)
38. D. Anderson, T. W. Yu, B. J. Phillips, P. Schmezer, *Mutat. Res.-Fund. Mol. M.* **307** (1994) 261 (<http://www.sciencedirect.com/science/article/pii/002751079490300X>)
39. D. Manojlović, M. D. Dramičanin, V. Miletić, D. Mitić-Ćulafić, B. Jovanović, B. Nikolić, *Dent. Mater.* **33** (2017) 454 (<http://www.sciencedirect.com/science/article/pii/S0109564117301525>)
40. I. A. Janković, Z. V. Šaponjić, E. S. Džunuzović, J. M. Nedeljković, *Nanoscale Res. Lett.* **5** (2010) 81 (<https://doi.org/10.1007/s11671-009-9447-y>)
41. J.-P. Cornard, C. Lapouge, *J. Phys. Chem., A* **110** (2006) 7159 (<https://doi.org/10.1021/jp060147y>)

42. S. Manzhos, K. Kotsis, *Chem. Phys. Lett.* **660** (2016) 69
(<https://www.cheric.org/research/tech/periodicals/view.php?seq=1495551>)
43. V. R. Coelho, C. G. Vieira, L. P. de Souza, L. L. da Silva, P. Pflüger, G. G. Regner, D. K. M. Papke, J. N. Picada, P. Pereira, *N.-S. Arch. Pharmacol.* **389** (2016) 1195
(<https://doi.org/10.1007/s00210-016-1281-z>).